



Electrochemical oxidation of anesthetic tetracaine in aqueous medium. Influence of the anode and matrix composition

Carlota Ridruejo^a, Claudio Salazar^b, Pere L. Cabot^a, Francesc Centellas^a, Enric Brillas^{a,*}, Ignasi Sirés^{a,*}

^a Laboratori d'Electroquímica dels Materials i del Medi Ambient, Departament de Química Física, Facultat de Química, Universitat de Barcelona, Martí i Franquès 1-11, 08028 Barcelona, Spain

^b Facultad de Ciencias Químicas, Laboratorio de Trazas Elementales y Especiación (LabTres), Universidad de Concepción, 4070371, Edmundo Larenas 129, Concepción, Chile

ARTICLE INFO

Article history:

Received 27 March 2017

Received in revised form 28 April 2017

Accepted 29 April 2017

Available online xxx

Keywords:

Active chlorine

BDD

Electrochemical oxidation

Hydroxyl radical

Tetracaine

Wastewater treatment

ABSTRACT

The degradation of 150 mL of 0.561 mM tetracaine hydrochloride at pH 3.0 by electrochemical oxidation with electrogenerated H₂O₂ (EO-H₂O₂) has been studied at a low current density of 33.3 mA cm⁻² in three different matrices: 0.050 M Na₂SO₄, real urban wastewater and a simulated matrix mimicking its electrolyte composition. Comparative trials were performed in an undivided cell with a 3 cm² boron-doped diamond (BDD), Pt, IrO₂-based or RuO₂-based anode and a 3 cm² air-diffusion cathode that allowed continuous H₂O₂ electrogeneration. In 0.050 M Na₂SO₄, much faster and overall removal of tetracaine occurred using BDD because of the large oxidation ability of BDD(OH) formed from anodic water oxidation. In either simulated matrix or real wastewater, the RuO₂-based anode yielded the quickest tetracaine decay due to a large production of active chlorine from anodic oxidation of Cl⁻. For the mineralization of the organic matter content, the BDD/air-diffusion cell was the best choice in all aqueous matrices, always reaching more than 50% of total organic carbon abatement after 360 min of electrolysis, as expected if BDD(OH) mineralizes more easily the chloroderivatives formed from tetracaine oxidation in the presence of active chlorine. The initial N of tetracaine was partly transformed into NO₃⁻, although the total nitrogen of all solutions always decayed by the release of volatile by-products. In the Cl⁻-containing matrices, significant amounts of ClO₃⁻ and ClO₄⁻ were obtained using BDD, whereas active chlorine was much largely produced using the RuO₂-based anode. Five aromatic by-products, one of them being chlorinated, along with low concentrations of oxalic acid were identified. The change in toxicity during EO-H₂O₂ with BDD in the sulfate and simulated matrices was also assessed.

© 2017.

1. Introduction

Thousands of tons of a large number of pharmaceuticals are consumed worldwide by humans and animals. Since they are not completely metabolized, they are continuously discharged into the environment via urine and feces. This mainly affects water bodies and, eventually, the quality of drinking water supplies. Despite their low contents at µg L⁻¹ level, the potential impact of pharmaceuticals on ecosystems and their long-term effects on the health of living beings have caused global alarm [1–4]. The occurrence of pharmaceuticals in water is explained by their incomplete removal by conventional physicochemical and biological treatments in wastewater treatment plants (WWTPs), thereby becoming persistent contaminants [3,4]. Tetracaine (2-dimethylaminoethyl-4-butylaminobenzoate, C₁₅H₂₄N₂O₂, M = 264.3 g mol⁻¹), commercially available as hydrochloride salt, is a potent local anesthetic belonging to the family of amino esters. It is used for topical anaesthesia in ophthalmology, spinal anaesthesia and nerve block and can be formulated as solu-

tions, creams, gels and as the base of ointments [5,6]. Its critical toxicity has been determined [7], and it has been detected in hospital wastewater with an average concentration of 0.48 µg L⁻¹ [8]. No previous work has reported the decontamination of water containing tetracaine. Research efforts are then necessary to show if this pharmaceutical can be destroyed in aqueous medium in order to prevent its toxic effects on living beings.

Advanced oxidation processes (AOPs) are powerful oxidation methods characterized by the continuous generation of reactive oxygen species (ROS) like hydroxyl radical (•OH). Since these species are formed in situ without addition of noxious chemicals, they are considered as eco-friendly technologies [9]. The very short lifetime of •OH (~10⁻⁹ s) and its very high standard reduction potential (E° = 2.8 V/SHE) allow its fast, non-selective reaction with most organics, showing a second-order rate constant (k₂) of 10⁷–10¹⁰ M s⁻¹, up to total mineralization in many cases [10,11]. For this reason, AOPs have got great interest for water remediation. Among these methods, electrochemical oxidation (EO) has been widely utilized as an electrochemical AOP (EAOP) that combines a large oxidation power with simplicity of use [11–13]. EO involves the destruction of organic pollutants in a free-chlorine aqueous medium through physisorbed hydroxyl radicals (M(OH)) originated at the surface of an

* Corresponding authors.

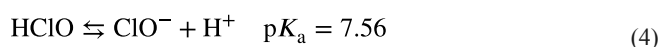
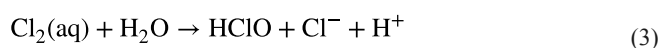
Email addresses: brillas@ub.edu (E. Brillas); i.sires@ub.edu (I. Sirés)

anode M from water oxidation [13–15]:

(1)

The nature of the anode has major influence on the oxidation ability of EO. Materials such as Pt and dimensionally stable anodes (DSA®) based on IrO₂ and RuO₂ behave as active anodes with low production of physisorbed M([•]OH) since it is transformed into an less powerful superoxide (M[•]O) species [13,16–20]. In contrast, large amounts of physisorbed M([•]OH) are formed at non-active anodes with large O₂-overvoltage. It has been found that boron-doped diamond (BDD) thin-film electrodes are the most powerful among the latter ones, having high corrosion stability in harsh media and hampering a strong adsorption of [•]OH on their surface. BDD allows a large degree of mineralization of aromatics including pharmaceuticals [14,15,19–31], with much quicker removal compared to that obtained using traditional anodes such as Pt [32,33] and PbO₂ [34].

The situation is very different if EO is performed in a chlorinated medium, since active chlorine species (Cl₂, HClO and/or ClO⁻) are produced from Cl⁻ oxidation at the anode [9,11–13]:



Under these conditions, physisorbed M([•]OH) and active chlorine species compete to oxidize the organic matter. It has been found that active DSA® anodes, pre-eminently RuO₂-based ones, yield larger quantity of active chlorine that can attack rapidly the aromatic structures, even more quickly than BDD([•]OH) [20,36]. However, highly persistent chloroderivatives are usually accumulated, giving rise to partial mineralization of solutions.

The EO process can be alternatively applied using continuous generation of H₂O₂ from the two-electron cathodic reduction of injected O₂ or air via reaction (5) [12,35–37], giving rise to the so-called EO with electrogenerated H₂O₂ (EO-H₂O₂) process:



Several carbonaceous cathodes such as activated carbon fiber [38], carbon nanotubes [39], carbon felt [40,41] and carbon-polytetrafluoroethylene (PTFE) gas-diffusion composites [20,42,43] have shown good performance for H₂O₂ generation from reaction (5).

In EO-H₂O₂, the electrogenerated H₂O₂ is partly destroyed to O₂ at the anode M yielding the hydroperoxyl radical M(HO₂[•]) from reaction (6) [11]:

(6)

and hence, organics can be removed by different ROS, being M([•]OH) much more powerful than H₂O₂ and M(HO₂[•]). In our laboratory, we have shown the potential applicability of EO-H₂O₂ to degrade some pharmaceuticals with a carbon-PTFE air-diffusion cathode

[20,33,43]. This cathode has been chosen since it is the most effective for O₂ reduction from reaction (5), avoiding the possible cathodic reduction of organics.

This work aims to assess the oxidation ability of EO-H₂O₂ to destroy tetracaine using an undivided cell with an air-diffusion cathode. The degradation was comparatively performed in pure sulfate medium, as well as in a simulated matrix with chloride + sulfate ions as model electrolytes to better understand its further destruction in a real wastewater matrix that contained large amounts of both ions along with natural organic matter (NOM, which mainly includes humic, fulvic and tannic acids). A pH of 3.0 was chosen to compare the present results with those obtained under similar conditions using Fenton-based EAOPs in future work. Four anodes including BDD, Pt, IrO₂-based and RuO₂-based were tested to establish the best electrolytic system. The pharmaceutical decay and mineralization rate were studied for each system and matrix. Primary by-products were identified by gas chromatography-mass spectrometry (GC-MS). Final carboxylic acids were detected by ion-exclusion high-performance liquid chromatography (HPLC) and the change in toxicity was determined from the standard method based on the change in bioluminescence of *Vibrio fischeri* bacteria.

2. Materials and methods

2.1. Reagents

Tetracaine hydrochloride (>99% purity), oxalic acid dihydrate (99% purity) and fumaric acid (99% purity) were supplied by Sigma-Aldrich. Na₂SO₄, NaCl, NH₄Cl, K₂SO₄ and NaNO₃, used as background electrolytes, were of analytical grade from Panreac, Probus and Prolabo. Synthetic and analytical solutions were prepared with ultrapure water obtained from a Millipore Milli-Q system with resistivity >18 MΩ cm at 25 °C. The initial pH was adjusted to 3.0 with analytical grade H₂SO₄ for sulfate solutions and analytical grade HClO₄ for the other water matrices, both of them supplied by Merck. All the other reagents and solvents needed for analysis were of analytical or HPLC grade purchased from Panreac and Merck.

2.2. Aqueous matrices

The electrolytic experiments were performed with three different aqueous matrices:

- (i) A real wastewater was obtained from the secondary effluent of a WWTP located in Gavà-Viladecans (Barcelona, Spain) that treats ca. 50,000 m³ d⁻¹ of urban and selected industrial wastewater. The samples were preserved in a refrigerator at 4 °C before use. Its main characteristics were: pH 8.1, specific conductivity of 1.73 mS cm⁻¹, 12.2 mg L⁻¹ of total organic carbon (TOC); cations concentration: 212 mg L⁻¹ Na⁺, 34 mg L⁻¹ K⁺, 86 mg L⁻¹ Ca²⁺, 24 mg L⁻¹ Mg²⁺, 0.19 mg L⁻¹ Fe²⁺ and 36.9 mg L⁻¹ NH₄⁺; anions content: 141.3 mg L⁻¹ SO₄²⁻, 318 mg L⁻¹ Cl⁻, 0.85 mg L⁻¹ NO₃⁻ and 0.79 mg L⁻¹ NO₂⁻.
- (ii) A simulated matrix mimicking the above ionic content, but without organic load, was prepared in ultrapure water. It was composed of 0.80 mM Na₂SO₄, 10 mM NaCl, 1.5 mM NH₄Cl, 0.5 mM K₂SO₄ and 0.02 mM NaNO₃, yielding pH 5.1 and conductivity of 1.79 mS cm⁻¹.
- (iii) A synthetic solution with 0.050 M of a typical non-chlorinated electrolyte such as Na₂SO₄, yielding pH 7.0 and conductivity of 6.89 mS cm⁻¹, was used for comparison.

Once the solution pH was adjusted to 3.0 in all cases, the conductivity rose up to 2.22, 2.01 and 7.53 mS cm⁻¹ for the real wastewater,

simulated matrix and sulfate solution, respectively. These values only varied slightly during all the EO-H₂O₂ processes tested.

2.3. Electrochemical system

The EO-H₂O₂ treatment of all tetracaine hydrochloride solutions was conducted with a conventional two-electrode, one-compartment glass tank reactor containing 150 mL of solution, which was vigorously stirred with a magnetic bar at 800 rpm. The cell was surrounded with a jacket for water recirculation through a thermostat to regulate the solution temperature to 35 °C. Four anodes of 3 cm² area were alternately tested: (i) a boron-doped diamond (BDD) thin film over Si substrate supplied by NeoCoat (Le-Chaux-de-Fonds, Switzerland), (ii) a Pt sheet of 99.99% purity supplied by SEMPSA (Barcelona, Spain), (iii) an IrO₂-based plate and (iv) a RuO₂-based plate, the two latter being supplied by NMT Electrodes (Pinetown, South Africa). The cathode was always a 3 cm² carbon-PTFE air-diffusion electrode purchased from Sainergy Fuel Cell (Chennai, India). It was mounted as described elsewhere [22] and continuously produced H₂O₂ upon air feeding at flow rate of 1 L min⁻¹. The distance between the anode and cathode was kept to about 1 cm. Trials were performed under galvanostatic conditions by using a constant current density (*j*) provided by an Amel 2049 potentiostat-galvanostat. The cell voltage was measured with a Demestres 601BR digital multimeter. Before the electrolytic treatment of the pharmaceutical solutions, the surface of all electrodes was electrochemically cleaned/activated by polarization in 0.050 M Na₂SO₄ at *j* = 100 mA cm⁻² for 180 min.

2.4. Analytical procedures

The electrical conductance and pH of solutions were measured on a Metrohm 644 conductometer and a Crison GLP 22 pH-meter, respectively. Prior to analysis, the samples were filtered with 0.45 μm PTFE membrane filters supplied by Whatman. H₂O₂ content in electrolyzed synthetic solutions was obtained from the light absorption of its Ti(IV) complex at λ = 408 nm, measured on an Unicam UV/Vis spectrophotometer at 25 °C [44]. Active chlorine concentration was determined by the *N,N*-diethyl-*p*-phenylenediamine colorimetric method at λ = 515 nm using a Shimadzu 1800 UV/Vis spectrophotometer [45].

The TOC content of the pharmaceutical solutions with ±1% accuracy was measured by injecting 50 μL aliquots into a Shimadzu VCSN TOC analyzer. Total nitrogen (TN) was obtained with a Shimadzu TNM-1 unit coupled to the above analyzer.

The tetracaine abatement and the evolution of generated carboxylic acids were followed by reversed-phase and ion-exclusion HPLC, respectively. These analyses were made upon injection of 10 μL aliquots into a Waters 600 LC coupled with a Waters 996 photodiode array detector. For reversed-phase HPLC, the LC was fitted with a BDS Hypersil C18 (250 mm × 4.6 mm) column at room temperature. A 50:50 (v/v) acetonitrile:water (KH₂PO₄ 10 mM, pH 3) at 1.0 mL min⁻¹ was used as mobile phase, detecting the peak of tetracaine (λ = 311 nm) at retention time (*t_r*) of 8.9 min. For ion-exclusion HPLC, a Bio-Rad Aminex HPX 87H (300 mm × 7.8 mm) column at 35 °C was employed, whereas the mobile phase was 4 mM H₂SO₄ eluted at 0.6 mL min⁻¹. The recorded chromatograms displayed peaks related to oxalic (*t_r* = 6.8 min) and fumaric (*t_r* = 14.7 min) acids at λ = 210 nm.

The concentration of metal cations in the real wastewater was obtained by inductively coupled plasma-optical emission spectroscopy (IPC-OES), whereas the NH₄⁺ concentration was obtained through the standard indophenol blue method using an Alpkem Flow Solution

IV flow injection system. The Cl⁻, ClO₃⁻, ClO₄⁻, NO₃⁻ and SO₄²⁻ contents in initial and treated synthetic solutions were determined by ion chromatography upon injection of 20 μL aliquots into a Kontron 465 LC fitted with a Waters IC-pack (150 mm × 4.6 mm) anion column at 35 °C, coupled with a Waters 432 conductivity detector. The mobile phase for this analysis was a solution of boric acid, sodium gluconate, sodium tetraborate, acetonitrile, butanol and glycerine eluted at 2 mL min⁻¹ (EPA 9056).

Stable aromatic by-products originated at 30 and 120 min of EO-H₂O₂ treatment of 0.561 mM of tetracaine hydrochloride in 0.050 M Na₂SO₄ and simulated matrix with a BDD/air-diffusion cell at *j* = 33.3 mA cm⁻² were identified by means of GC-MS using a NIST05 data library. The organics accumulated in electrolyzed samples were concentrated by solid-phase extraction through repeated uptake using Agilent Bond Elute OMIX SPE pipette tips, followed by extraction with 2 mL of methanol as eluent. The GC-MS analysis was made with an Agilent Technologies 6890 N GC fitted with a non-polar Teknokroma Sapiens-X5 ms (0.25 μm, 30 m × 0.25 mm) column and coupled with an Agilent Technologies 5975C MS, which operated in electron impact mode at 70 eV. A temperature ramp of 36 °C for 1 min, 5 °C min⁻¹ up to 325 °C and hold time 10 min was applied, setting temperatures of 250, 230 and 300 °C for the inlet, source and transfer line, respectively.

The toxicity of untreated and treated tetracaine hydrochloride solutions was determined as the effective concentration that reduces 50% of the bioluminescence intensity of *Vibrio fischeri* marine bacteria after 15 min of exposure at 25 °C (EC₅₀, in mg L⁻¹) using an AFNOR T90-301 Microtox® system. The bioluminescent bacteria and other reagents were provided by Modern Water (New Castle, USA) and the analysis was conducted following the standard Microtox® test recommended by the manufacturer. Each sample was adjusted to pH 7.0 prior to measurement.

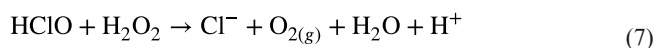
3. Results and discussion

3.1. Tetracaine decay with different anodes and aqueous matrices

Considering the very low conductivity of the simulated matrix and real wastewater, preliminary tests were made to ascertain the maximum *j* value that could be employed for comparison between the different electrolytic systems in EO-H₂O₂ under the present experimental conditions. The trials were performed once the pH of both wastewater samples was adjusted to 3.0 with HClO₄, which was employed as inert electrolyte to prevent interference with their sulfate + chloride content, which determines the oxidation ability of this EAOP [9,11]. The maximum *j* was established as 33.3 mA cm⁻², corresponding to a current of 100 mA, since it gave rise to a cell voltage ca. 25 V for the simulated matrix in the BDD/air-diffusion cell. A higher voltage would be detrimental for the stability of the carbonaceous cathode and thus, this *j* value was utilized in all subsequent assays.

Firstly, the ability for H₂O₂ electrogeneration in the different matrices at pH 3.0 in the absence of pharmaceutical was examined using the BDD/air-diffusion cell at 33.3 mA cm⁻² for 360 min. No significant change in solution pH was observed during these runs. At the end of the electrolysis, H₂O₂ was accumulated up to 34.0 mM in the 0.050 M Na₂SO₄ solution, 31.2 mM in the simulated matrix and 25.1 mM in the real wastewater. Taking into account that the Faraday's law predicts a maximum accumulation of 74.6 mM H₂O₂ under such conditions, the 46% of current efficiency found to produce this species in the 0.050 M Na₂SO₄ solution is indicative of its significant disappearance from reaction (6) originating the weak radical BDD(HO₂[•]) that is formed in concomitance with BDD(OH) gener-

ated from reaction (1) [9,20]. The lower accumulation of H_2O_2 in the simulated matrix can be ascribed to its partial destruction through an additional waste reaction with HClO , the pre-eminent active chlorine species formed at pH 3.0 [11–13], as follows:



The larger H_2O_2 decay in the real wastewater compared to the other two matrices suggests the additional attack of this species on the NOM contained in it. One can thus infer that H_2O_2 will be also able to remove some organic load during the EO- H_2O_2 treatment of tetracaine hydrochloride spiked into real wastewater, as described below.

Once clarified the behavior of the electrolytic systems, the decay of 0.561 mM tetracaine in the three aqueous matrices with each of the four anodes was followed by reversed-phase HPLC for 360 min as maximal. In all these trials, the initial pH of 3.0 decayed slightly with time up to final values close to 2.7–2.8, suggesting the formation of acidic by-products from pharmaceutical degradation. In the 0.050 M Na_2SO_4 solution, Fig. 1a highlights the total disappearance of the pharmaceutical using the BDD anode after about 300 min of treatment. In contrast, the tetracaine concentration was reduced by only 60.2%, 50.3% and 59.3% with Pt, IrO_2 -based and RuO_2 -based anodes, respectively. Consequently, the oxidation ability of the anodes

in this medium increased in the order: IrO_2 -based < RuO_2 -based \sim Pt \ll BDD. This trend agrees with the expected oxidative superiority of the non-active BDD anode over the other three active ones [13–15], owing to the larger generation of physisorbed $\text{M}(\cdot\text{OH})$ from reaction (1). A similar tendency has been reported for the degradation of 100 mL of 1.04 mM methylparaben using the same kind of anodes under analogous conditions but at $j = 66.7 \text{ mA cm}^{-2}$ [43].

The good linear fittings obtained from the pseudo-first-order kinetic analysis of the above concentration decays are presented in Fig. 1b. Increasing apparent rate constants (k_1) of $1.90 \times 10^{-3} \text{ min}^{-1}$ (square of the correlation coefficient, $R^2 = 0.982$) for IrO_2 -based, $2.39 \times 10^{-3} \text{ min}^{-1}$ ($R^2 = 0.985$) for RuO_2 -based, $2.50 \times 10^{-3} \text{ min}^{-1}$ ($R^2 = 0.998$) for Pt and $1.15 \times 10^{-2} \text{ min}^{-1}$ ($R^2 = 0.992$) for BDD were obtained. As can be seen, the attack of BDD($\cdot\text{OH}$) onto tetracaine was 4.6-fold, 1.8-fold and 6.0-fold faster than that of Pt($\cdot\text{OH}$), RuO_2 ($\cdot\text{OH}$) and IrO_2 ($\cdot\text{OH}$). Hence, these three ROS are produced to a much lesser extent, which corroborates the superior oxidation ability of BDD in sulfate medium [18–20]. This behavior suggests the removal of tetracaine by a small, constant amount of physisorbed radicals during the EO- H_2O_2 treatment.

The destruction of the pharmaceutical became much quicker when the aqueous mixture contained Cl^- , which can be observed in Fig. 2a in the case of the simulated matrix. Tetracaine disappeared in shorter times of about 60 min for Pt and IrO_2 -based, 40 min for BDD and

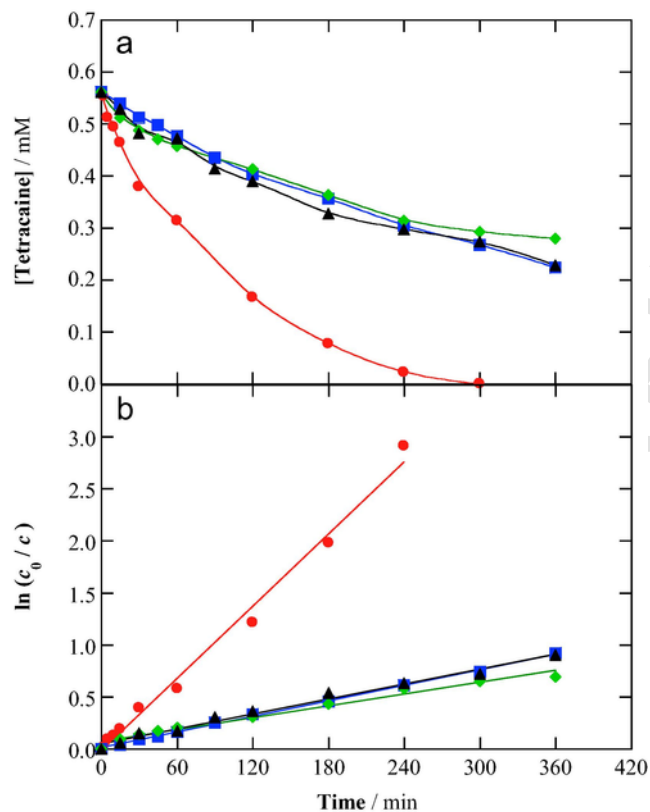


Fig. 1. (a) Concentration decay of tetracaine with electrolysis time for the electrochemical oxidation with electrogenerated H_2O_2 (EO- H_2O_2) treatment of 150 mL of a 0.561 mM tetracaine hydrochloride solution in 0.050 M Na_2SO_4 at pH 3.0 and 35 °C using a stirred tank reactor with an air-diffusion cathode at current density (j) of 33.3 mA cm^{-2} . Anode: (●) Boron-doped diamond (BDD), (■) Pt, (◆) IrO_2 -based and (▲) RuO_2 -based. The area of all electrodes was 3 cm^2 . (b) Pseudo-first-order kinetic analysis of the concentration decays.

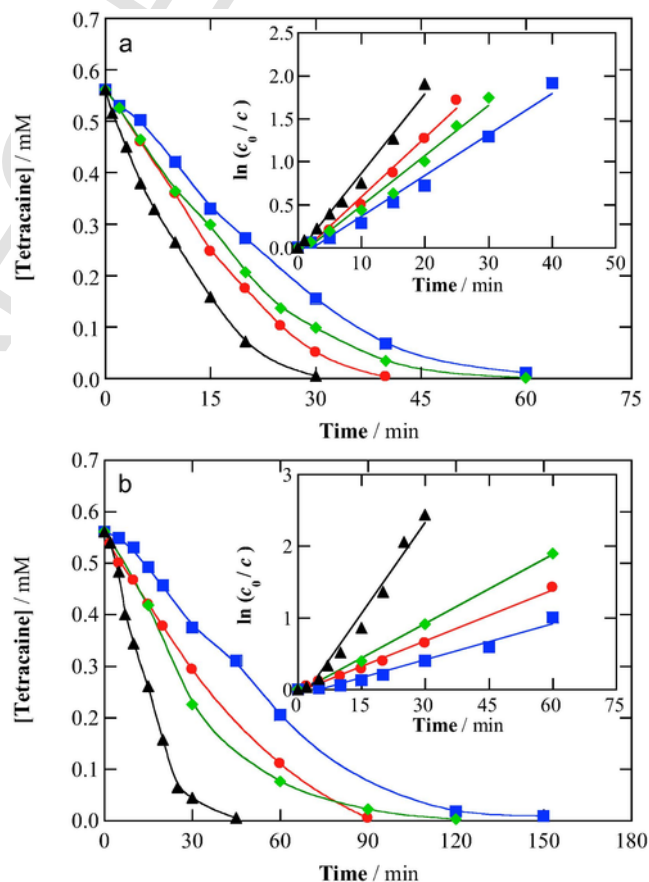


Fig. 2. Time course of tetracaine concentration for the degradation of 150 mL of 0.561 mM of the pharmaceutical spiked into (a) a simulated matrix and (b) real wastewater, at pH 3.0 and 35 °C by EO- H_2O_2 at $j = 33.3 \text{ mA cm}^{-2}$. Anode: (●) BDD, (■) Pt, (◆) IrO_2 -based and (▲) RuO_2 -based. The inset panels present the corresponding kinetic analysis considering a pseudo-first-order decay for tetracaine.

30 min for RuO₂-based, revealing that the oxidation power in this medium rose in the sequence: IrO₂-based < Pt < BDD < RuO₂-based. Accordingly, from the pseudo-first-order kinetic analysis of the concentration abatements depicted in the inset panel shown in Fig. 2a, raising k_1 values of $4.75 \times 10^{-2} \text{ min}^{-1}$ ($R^2 = 0.982$), $5.82 \times 10^{-2} \text{ min}^{-1}$ ($R^2 = 0.982$), $6.86 \times 10^{-2} \text{ min}^{-1}$ ($R^2 = 0.989$) and $9.22 \times 10^{-2} \text{ min}^{-1}$ ($R^2 = 0.987$) for IrO₂-based, Pt, BDD and RuO₂-based, respectively, were found. The most powerful anode in this medium was that made of RuO₂, which clearly outperformed the other three materials. Compared with the k_1 -values determined in 0.050 M Na₂SO₄, the degradation rate using RuO₂ presented a 38-fold enhancement, similar to that of Pt and IrO₂-based, whereas in the case of BDD only a 5.96-fold acceleration was found. The enhanced removal of the pharmaceutical can be explained by the fast attack of active chlorine (HClO at pH 3.0) originated from reactions (2) and (3). Our results give evidence that active chlorine was produced extensively by active anodes, pre-eminently the RuO₂-based one, becoming the main oxidant for tetracaine. In contrast, active chlorine was formed to a smaller extent with BDD and thus, it competed with BDD([•]OH) to attack the pharmaceutical. The positive beneficial action of Cl⁻ ions, yielding active chlorine as a powerful oxidant, has been previously reported for the EO-H₂O₂ treatment of Ponceau 4R dye [19] using BDD and Pt anodes and of methylparaben [43] using the four kind of anodes.

The tetracaine abatement became slower when it was spiked into the real wastewater effluent, as can be seen in Fig. 2b and in the corresponding kinetic analysis of the inset panel. Total removal was achieved after 150, 120, 90 and 45 min using IrO₂-based, Pt, BDD and RuO₂-based anodes, with k_1 -values of $1.67 \times 10^{-2} \text{ min}^{-1}$ ($R^2 = 0.980$), $3.19 \times 10^{-2} \text{ min}^{-1}$ ($R^2 = 0.998$), $2.36 \times 10^{-2} \text{ min}^{-1}$ ($R^2 = 0.995$) and $8.45 \times 10^{-2} \text{ min}^{-1}$ ($R^2 = 0.981$). Although the RuO₂-based anode was again the most powerful one, its oxidation ability dropped compared with that found in the simulated matrix. Larger decreases were found for the other anodes, particularly for BDD, whose oxidation power was one third of the previous one. The slower destruction of tetracaine in the real wastewater can be ascribed to the parallel oxidation of NOM by generated M([•]OH) and active chlorine. This competition was less significant for the RuO₂-based anode, probably because of its greater ability to produce active chlorine, but it was comparatively important for the BDD anode, suggesting a dramatic scavenging effect of NOM on BDD([•]OH) with the consequently lower availability for the pharmaceutical.

3.2. Mineralization of tetracaine hydrochloride solutions

Once elucidated the effect of the anodes and aqueous matrices on pharmaceutical decay, the mineralization of solutions with 0.561 mM tetracaine hydrochloride at pH 3.0 and 35 °C was comparatively investigated for the different electrolytic systems at $j = 33.3 \text{ mA cm}^{-2}$ for 360 min. The normalized TOC removal with electrolysis time for such trials is presented in Fig. 3. Worth noting, one can observe that the most effective anode for mineralization was always BDD, regardless of the medium used.

Fig. 3a highlights that in 0.050 M Na₂SO₄, TOC was reduced by 52.9% at the end of EO-H₂O₂ treatment with BDD, whereas <7% of the organic load was mineralized using Pt, IrO₂-based or RuO₂-based anodes. This means that the strongest ROS generated under these conditions, i.e., BDD([•]OH), was powerful enough not only to remove the parent drug in 300 min (see Fig. 1a), but also to mineralize a large amount of its by-products. In contrast, generated Pt([•]OH), IrO₂([•]OH) and RuO₂([•]OH) turned out to be very inefficient to transform the intermediates into CO₂. This is not surprising based on the very slow

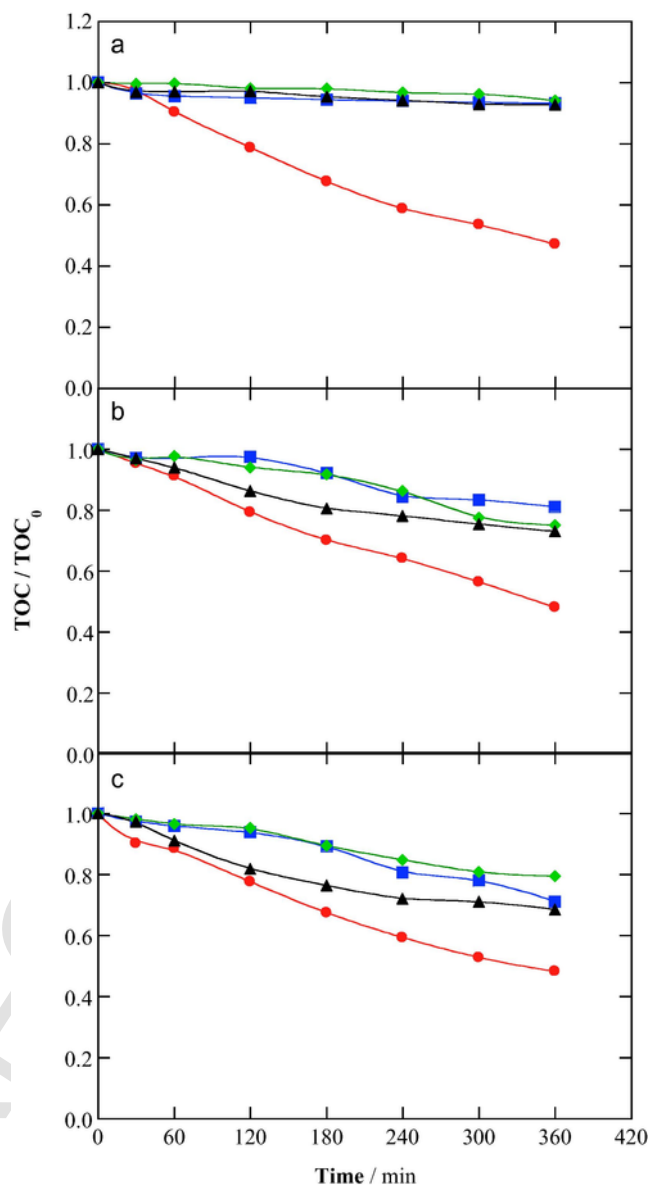


Fig. 3. Normalized TOC removal with electrolysis time for the EO-H₂O₂ assays made under the conditions described in: (a) Fig. 1a, (b) Fig. 2a and (c) Fig. 2b. Anode: (●) BDD, (■) Pt, (◆) IrO₂-based and (▲) RuO₂-based.

destruction of the pharmaceutical with the latter three anodes (see Fig. 1a).

In the simulated matrix (Fig. 3b), the mineralization ability of BDD was slightly lower, achieving 52.0% of TOC decay. Conversely, the mineralization degree was strongly upgraded with the three active anodes, which led to a TOC reduction of 19.1% (Pt), 25.0% (IrO₂-based) and 27.2% (RuO₂-based). Despite the clear superiority of the RuO₂-based anode to destroy tetracaine (see Fig. 2a) as result of the quicker attack of the greater amounts of generated active chlorine, the by-products formed, probably including chloroderivatives [9,11], became so recalcitrant that they were poorly mineralized. The same behavior can be valid for Pt and IrO₂-based as well, since they also generated active chlorine as the main oxidizing species in the simulated matrix. The greater mineralization achieved with BDD can then be accounted for by two factors: (i) the smaller formation of active chlorine species, with subsequent accumulation of a lower amount of

chloro-derivatives and, more important, (ii) the larger ability of BDD($\cdot\text{OH}$) to mineralize the intermediates formed.

The different reactivity of oxidizing species can also be observed in Fig. 3c, where the TOC of the electrolyzed pharmaceutical solution in real wastewater was finally reduced by 51.8%, 28.9%, 22.6% and 31.5% using BDD, Pt, IrO₂-based and RuO₂-based anodes, respectively. Note that the initial TOC of 0.561 mM tetracaine hydrochloride in the real wastewater was 112 mg L⁻¹, being a bit higher than 100 mg L⁻¹ TOC in the simulated matrix due to the existence of NOM in the former matrix. One can then conclude that a larger amount of organic matter was mineralized in the real water samples regardless of the anode (except for the IrO₂-based one) because of the competitive degradation of NOM and tetracaine by M($\cdot\text{OH}$) and active chlorine. Again, the oxidation power of physisorbed BDD($\cdot\text{OH}$) became greater than that of active chlorine and hence, EO-H₂O₂ with BDD was the most powerful decontamination treatment for solutions prepared in real wastewater.

3.3. Fate of inorganic ions and mineralization current efficiency

The evolution of TN and inorganic ions present in the water matrices and/or released along tetracaine cleavage was analyzed for the EO-H₂O₂ treatments after 360 min in 0.050 M Na₂SO₄ and in the simulated matrix, thus avoiding the expected interferences from NOM destruction in the real wastewater. In 0.050 M Na₂SO₄, only the behavior of the most potent anode (BDD) was investigated. It was found that the initial SO₄²⁻ content remained practically constant during the electrolysis, whereas the initial Cl⁻ concentration (from the hydrochloride) decayed from 0.561 mM to 0.222 mM, with a final amount of 6.39 mg L⁻¹ of active chlorine (0.12 mM). The very slow removal of tetracaine in this medium using the three active anodes (see Fig. 1) suggests a really poor contribution of active chlorine compared to M($\cdot\text{OH}$) and thus, it was correct to omit the role of Cl⁻ in this medium in sections 3.1 and 3.2. At the end of EO-H₂O₂, 0.27 mM NO₃⁻ (24.1% of initial N) and no NH₄⁺ or NO₂⁻ ions were found. Moreover, the TN value dropped from 1.12 to 0.96 mM. These findings indicate that 0.69 mM (61.6%) of the initial N of tetracaine still remained in the final solution as highly recalcitrant *N*-derivatives, with a loss of 14.3% of initial N probably due to the release of volatile N₂ and/or N_xO_y, as found for other nitrogenated aromatics [12,37].

Table 1 summarizes the results obtained for the initial solution and after 360 min of electrolysis using the four anodes tested in the simulated matrix. As can be seen, the TN dropped in all cases during the EO-H₂O₂ treatment due to the loss of volatile by-products, primarily for the RuO₂-based anode (release of 65.6% of initial N), which can be plausibly ascribed to the formation of chloramines by reaction of the large amounts of generated active chlorine with NH₄⁺

Table 1

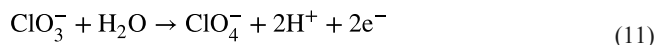
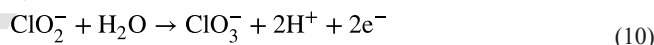
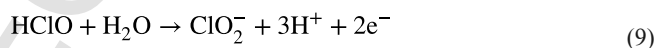
Total nitrogen, active chlorine and inorganic ions concentration before and after 360 min of EO-H₂O₂ treatment of 150 mL of a simulated aqueous matrix containing 0.561 mM tetracaine hydrochloride at pH 3.0 and 35 °C, using different anodes and an air-diffusion cathode at $j = 33.3 \text{ mA cm}^{-2}$.

	Before electrolysis	BDD (end)	Pt (end)	IrO ₂ -based (end)	RuO ₂ -based (end)
TN (mM)	2.62	2.06	2.09	2.27	0.90
NO ₃ ⁻ (mM)	0.020	0.034	0.044	0.060	0.091
SO ₄ ²⁻ (mM)	1.51	1.20	1.50	1.51	1.40
Cl ⁻ (mM)	14.82	2.38	10.63	14.45	7.51
ClO ₃ ⁻ (mM)	–	6.64	2.37	0.02	0.38
ClO ₄ ⁻ (mM)	0.55	1.94	1.00	0.73	0.72
Active chlorine (mg L ⁻¹)	–	2.07	1.57	3.14	65.25

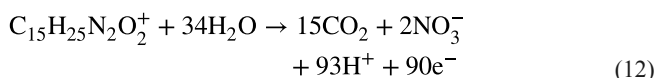
contained in the matrix. Table 1 also shows the release of NO₃⁻ from tetracaine under all conditions, with increasing contents of 0.014, 0.024, 0.040 and 0.071 mM using BDD, Pt, IrO₂-based and RuO₂-based anodes, respectively. This trend is indicative of the presence of much lower amounts of *N*-derivatives in the final solutions using the three active anodes compared to BDD, which can be related to the preferential destruction of these by-products by active chlorine, rather than by BDD($\cdot\text{OH}$). In contrast, the initial SO₄²⁻ decreased much more largely for BDD. This can be explained by its anodic oxidation to peroxodisulfate (S₂O₈²⁻), favored at the BDD surface as follows [9,13]:



The fate of detected chlorinated ions is also remarkable. From Table 1, one can infer that the initial Cl⁻ was much more rapidly removed using BDD, which could seem contradictory from the results reported in Figs. 2 and 3 that have been explained on the basis of the large effectiveness of generated active chlorine formed with the three active anodes. The larger destruction of Cl⁻ with BDD can then be ascribed to the quicker consecutive oxidation of active chlorine to ClO₃⁻ and ClO₄⁻, according to reactions (9)(11) [37,43]. Table 1 shows a much greater production of the two latter ions using BDD. Furthermore, the remaining active chlorine rose in the sequence: Pt < BDD < IrO₂-based ≪ RuO₂-based, i.e., the same order followed to degrade tetracaine in Fig. 2a, which corroborates the pre-eminent oxidative role of this species in Cl⁻-containing matrices. Note the active chlorine concentration as high as 65.25 mg L⁻¹ found with the RuO₂-based anode, whereas it was < 3.5 mg L⁻¹ with the other ones. This agrees with the expected greater ability of the former anode to oxidize Cl⁻, pointed out above, with low formation of ClO₃⁻ and ClO₄⁻ [13,43].



Based on the aforementioned findings, the theoretical mineralization reaction of the protonated form of tetracaine, the species present in each matrix, can be written as reaction (12), with formation of CO₂ and NO₃⁻ and the consumption of 90 electrons (n):



The mineralization current efficiency (MCE) for each trial at applied current I (=0.100 A) and given electrolysis time t (in h) was then estimated from Eq. (13) [27,33]:

$$\% \text{MCE} = \frac{n F V_s \Delta(\text{TOC})_{\text{exp}}}{4.32 \times 10^7 m I t} \times 100 \quad (13)$$

where F is the Faraday constant (96,487 C mol⁻¹), V_s is the solution

volume ($=0.150\text{ L}$), $\Delta(\text{TOC})_{\text{exp}}$ is the experimental TOC abatement (in mg L^{-1}), 4.32×10^7 is a conversion factor ($3600\text{ s h}^{-1} \times 12,000\text{ mg C mol}^{-1}$) and m is the number of carbon atoms of tetracaine ($=15$).

Fig. 4a and b depict the MCE values calculated from Eq. (13) for the assays shown in Fig. 3a and b, respectively. In both cases, the current efficiency for BDD fluctuates between 17.7% and near 21% at 60–360 min of electrolysis, being slightly higher in the 0.050 M Na_2SO_4 compared with the simulated matrix. This means that organic pollutants were mineralized at practically constant rate during each run, independently of the main oxidizing species, which was $\text{BDD}(\cdot\text{OH})$ in the former matrix and its combination with active chlorine in the second one. Conversely, the MCE values using the three active anodes changed strongly depending on the absence or presence of Cl^- . In 0.050 M Na_2SO_4 , owing to a low oxidation ability of their physisorbed $\text{M}(\cdot\text{OH})$, the current efficiency was very small attaining final values of about 2% for the three anodes. However, the current efficiency was much greater in the simulated matrix thanks to the additional oxidation power of generated active chlorine, and it varied between 5.9% and 7.9% using Pt, 6.0%–9.0% with IrO_2 -based and between 9.0%–13.8% with a RuO_2 -based anode, suggesting an almost constant mineralization rate in this medium.

The above results allow concluding that the BDD/air-diffusion cell was the best system to decontaminate the sulfate solution, the simulated matrix and the real wastewater containing tetracaine. This is due to the great mineralization power of $\text{BDD}(\cdot\text{OH})$ alone or in combination with active chlorine, although the process became slightly less efficient in the presence of Cl^- because of the formation of persistent chloroderivatives, as discussed below.

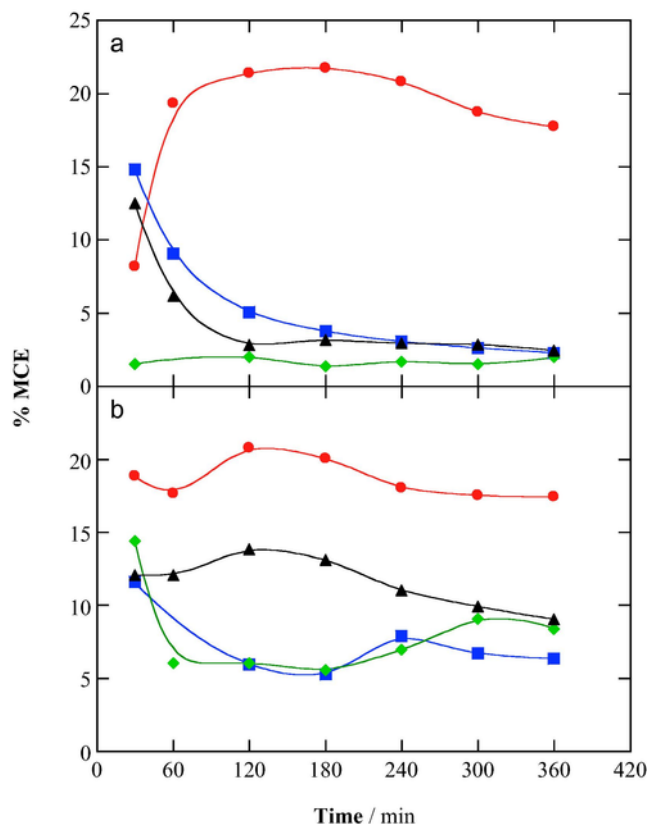


Fig. 4. Mineralization current efficiency calculated from Eq. (13) vs. electrolysis time for the profiles presented in: (a) Fig. 3a and (b) Fig. 3b.

3.4. Detection of by-products and toxicity assessment

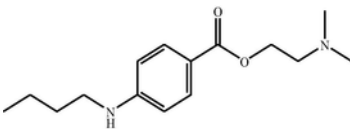
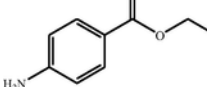
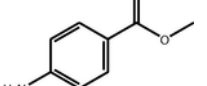
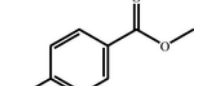
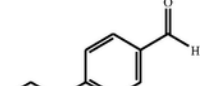
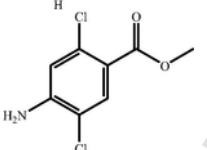
Table 2 summarizes the aromatic by-products identified by GC–MS for tetracaine (**1**) in 0.050 M Na_2SO_4 and in the simulated matrix at pH 3.0 upon degradation by the best $\text{EO-H}_2\text{O}_2$ treatment, i.e., using BDD anode at $j = 33.3\text{ mA cm}^{-2}$. Up to four intermediates (compounds **2a–5a**) were detected in the former medium. Compound **2a** is originated from the loss of both, the butyl group of the secondary amine of **1** and a dimethylamine side group. Further release of a side methyl group of the ethyl ester yields compound **3a**, whose $-\text{NH}_2$ group can be subsequently oxidized to $-\text{NO}_2$ yielding compound **4a**. On the other hand, the loss of the ethyl group of the secondary amine of **1** and the cleavage of the carboxylate one leads to compound **5a**. All these aromatic came from the successive attack of the preferential oxidant $\text{BDD}(\cdot\text{OH})$ onto **1**, but they were not found during the $\text{EO-H}_2\text{O}_2$ treatment in the simulated matrix. Under these conditions, Table 2 shows the detection of only the dichloroaromatic **2b**, thus corroborating the destruction of **1** by means of active chlorine formed from the anodic oxidation of Cl^- of the medium and the generation of recalcitrant chloroderivatives, as proposed above.

Along the degradation of aromatic pollutants by $\text{EO-H}_2\text{O}_2$, the cleavage of the benzene rings of aromatic intermediates to yield final short-chain linear aliphatic carboxylic acids is expected [9–12,40–43]. This behavior was confirmed for tetracaine from ion-exclusion HPLC analysis of 0.561 mM drug solutions electrolyzed using the potent BDD/air-diffusion cell. Fig. 5 shows that, in 0.050 M Na_2SO_4 , oxalic acid was gradually accumulated up to attain a concentration of 0.025 mM, whereas very small contents $<6.0 \times 10^{-4}\text{ mM}$ fumaric acid were also detected. It is well known that fumaric acid is oxidized to oxalic acid as ultimate by-product, which is slowly and directly transformed into CO_2 at the BDD surface [11,12]. Note that the final concentrations of both acids only accounted for 0.6 mg L^{-1} (1.3%) out of the 47.1 mg L^{-1} TOC of the final electrolyzed solution (see Fig. 3a), indicating that a great deal of remaining organic matter corresponded to other unidentified compounds, including *N*-derivatives, as suggested above. For the simulated matrix, Fig. 5 only highlights the presence of oxalic acid, with contents $<3.5 \times 10^{-3}\text{ mM}$ ($<0.1\text{ mg L}^{-1}$ TOC). Such a low amount suggests that chloroderivatives originated from this matrix were rather oxidized to short-chain by-products different from simple, non-chlorinated carboxylic acids to be mineralized to CO_2 .

The relative toxicity of generated intermediates was assessed from the change in EC_{50} of solutions degraded by $\text{EO-H}_2\text{O}_2$ with a BDD anode. As can be seen in Fig. 6, the value of this parameter for 0.561 mM tetracaine hydrochloride in the sulfate solution was 2.35 mg L^{-1} , being slightly lower (1.46 mg L^{-1}) in the real wastewater due to some toxic compounds related to its NOM content. These EC_{50} values grew up to 7.05 and 2.68 mg L^{-1} at the end of electrolysis, respectively, suggesting a very low loss of toxicity of both treated matrices. To better clarify this behavior, the same matrices but with smaller content of 0.056 mM tetracaine hydrochloride ($\sim 10\text{ mg L}^{-1}$ TOC) were electrolyzed under analogous conditions for 360 min, achieving 46.1% and 62.7% of mineralization. Fig. 6 depicts a dramatic drop of the starting $\text{EC}_{50} = 20.35\text{ mg L}^{-1}$ of the 0.056 mM tetracaine hydrochloride in 0.050 M Na_2SO_4 solution to 4.78 mg L^{-1} at 180 min, followed by a slight increase to 6.30 mg L^{-1} at 360 min. Similarly, the lower EC_{50} of the real wastewater (17.73 mg L^{-1}) decayed more largely, up to 0.65 mg L^{-1} at 240 min, and attained a final value of 2.08 mg L^{-1} . These findings indicate that the by-products formed during both $\text{EO-H}_2\text{O}_2$ treatments were more toxic than the parent drug, showing higher toxicity in the real waste-

Table 2

Characteristics of the aromatic by-products of tetracaine (**1**) identified by GC–MS during the EO-H₂O₂ degradation of 150 mL of 0.561 mM tetracaine hydrochloride, in 0.050 M Na₂SO₄ (compounds **2a–5a**) or in a simulated matrix (compound **2b**), at pH 3.0 and 35 °C with a BDD/air-diffusion cell at $j = 33.3 \text{ mA cm}^{-2}$.

Reference	Compound	Molecular structure	t_r^a (min)	Main fragmentation ions (m/z)
1	Tetracaine		41.1	210, 139, 71, 58
2a	4-Aminobenzoic acid ethyl ester		7.23	165, 149, 135, 120
3a	4-Aminobenzoic acid methyl ester		7.60	151, 133, 119, 105, 77
4a	4-Nitrobenzoic acid methyl ester		33.65	181, 163, 149, 133, 104, 92, 76
5a	4-Ethylamino benzaldehyde		27.04	147, 135, 107, 94, 77
2b	4-Amino-2,5-dichlorobenzoic acid methyl ester		29.05	219, 188, 160, 124

^a Retention time.

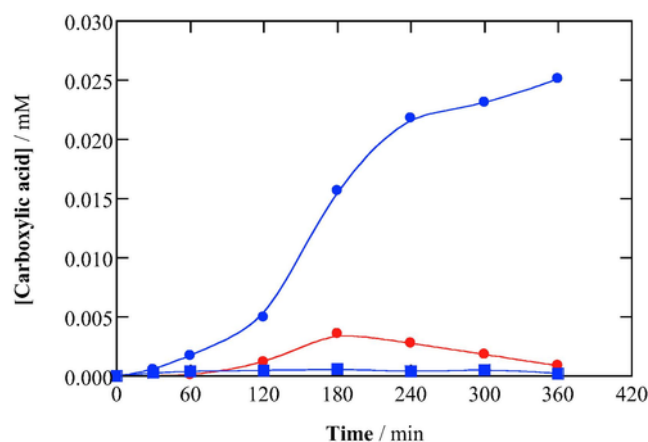


Fig. 5. Evolution of the concentration of (●●) oxalic and (■) fumaric acids detected during the EO-H₂O₂ treatment of 150 mL of 0.561 mM tetracaine hydrochloride in: (●●) 0.050 M Na₂SO₄ and (●●) simulated matrix, at pH 3.0 and 35 °C using a BDD/air-diffusion cell at $j = 33.3 \text{ mA cm}^{-2}$.

water because of the production of a large amount of chloroderivatives. Therefore, longer electrochemical treatments would be required in case of implementation of the EO-H₂O₂ process, aiming to ensure complete detoxification.

4. Conclusions

The removal of tetracaine in 0.050 M Na₂SO₄ solution by EO-H₂O₂ was much faster using BDD than active anodes like Pt,

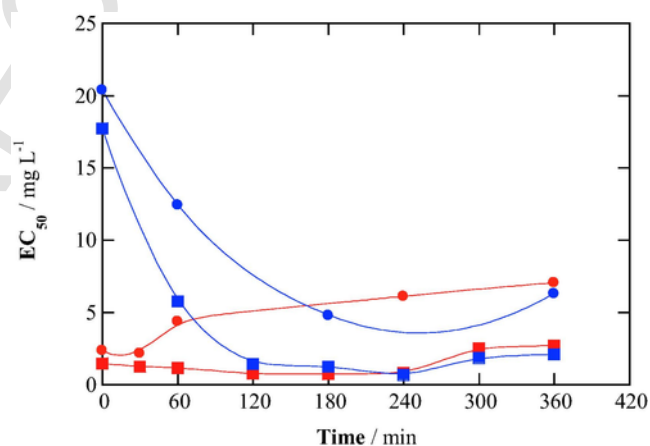
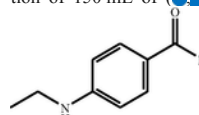


Fig. 6. Time course of EC₅₀ determined from the abatement at 15 min of the bioluminescence of the marine bacteria *Vibrio fischeri* during the EO-H₂O₂ degradation of 150 mL of (●●) 0.056 and (●●) 0.561 mM tetracaine hydrochloride in: (●●) 0.050 M Na₂SO₄ and (■) real wastewater. All trials



were performed at pH 3.0 and 35 °C using a BDD/air-diffusion cell at $j = 33.3 \text{ mA cm}^{-2}$.

IrO₂-based and RuO₂-based ones, due to the greater oxidation ability of BDD(·OH) compared to that of their M(·OH). In contrast, quicker pharmaceutical decay was found using the RuO₂-based anode in the simulated matrix and the real wastewater, because this material pro-

duces greater amounts of active chlorine that attack very rapidly the parent molecule. Regarding the mineralization of tetracaine solutions, the BDD/air-diffusion cell became the best system regardless of the matrix, leading to about 52% of TOC removal after 360 min at $j = 33.3 \text{ mA cm}^{-2}$. This means that BDD(OH) is able to gradually mineralize the chlorinated by-products that are typical in Cl^- -containing matrices. The initial N of tetracaine was transformed into NO_3^- , *N*-derivatives and volatile by-products, whereas the Cl^- ion was mainly converted to ClO_3^- and ClO_4^- ions with BDD and to active chlorine with the active anodes, especially with the RuO_2 -base one. Up to four aromatic intermediates were detected in 0.050 M Na_2SO_4 , whereas in the simulated matrix a dichloroaromatic was identified, corroborating the formation of chloroderivatives under real conditions. This agrees with the significant decrease of EC_{50} values found in all the trials performed in this work.

Acknowledgements

Financial support from project CTQ2016-78616-R (AEI/FEDER, EU) and from the FPI grant awarded to C. Ridruejo (MINECO, Spain) is acknowledged. C. Salazar thanks FONDECYT Postdoctoral Grant 3150253 (Chile).

References

- I. Sirés, E. Brillas, Remediation of water pollution caused by pharmaceutical residues based on electrochemical separation and degradation technologies: a review, *Environ. Int.* 40 (2012) 212–229.
- L. Feng, E.D. Van Hullebusch, M.A. Rodrigo, G. Esposito, M.A. Oturan, Removal of residual anti-inflammatory and analgesic pharmaceuticals from aqueous systems by electrochemical advanced oxidation processes. A review, *Chem. Eng. J.* 228 (2013) 944–964.
- J. Rivera-Utrilla, M. Sánchez-Polo, M.A. Ferro-García, G. Prados-Joya, R. Ocampo-Pérez, Pharmaceuticals as emerging contaminants and their removal from water. A review, *Chemosphere* 93 (2013) 1268–1287.
- O. Golovko, V. Kumar, G. Fedorova, T. Randak, R. Grabic, Seasonal changes in antibiotics, antidepressants/psychiatric drugs, antihistamines and lipid regulators in a wastewater treatment plant, *Chemosphere* 111 (2014) 418–426.
- F. Al-Otaibi, E. Ghazaly, A. Johnston, D. Perrett, Development of HPLC-UV method for rapid and sensitive analysis of topically applied tetracaine: its comparison with a CZE method, *Biomed. Chromatogr.* 28 (2014) 826–830.
- J.P. Shubha, Puttaswamy, Oxidation of tetracaine hydrochloride by chloramine-b in acid medium: kinetic modeling, *Adv. Phys. Chem.* (2014). Article ID 238984, 8 pages.
- J. Fick, R.H. Lindberg, M. Tysklind, D.G.J. Larsson, Predicted critical environmental concentrations for 500 pharmaceuticals, *Regul. Toxicol. Pharmacol.* 58 (2010) 516–523.
- B.I. Escher, R. Baumgartner, M. Koller, K. Treyer, J. Lienert, C.S. McArdell, Environmental toxicology and risk assessment of pharmaceuticals from hospital wastewater, *Water Res.* 45 (2011) 75–92.
- I. Sirés, E. Brillas, M.A. Oturan, M.A. Rodrigo, M. Panizza, Electrochemical advanced oxidation processes: today and tomorrow. A review, *Environ. Sci. Pollut. Res.* 21 (2014) 8336–8367.
- S. Vasudevan, M.A. Oturan, Electrochemistry: as cause and cure in water pollution-an overview, *Environ. Chem. Lett.* 12 (2014) 97–108.
- C.A. Martínez-Huitile, M.A. Rodrigo, I. Sirés, O. Scialdone, Single and coupled electrochemical processes and reactors for the abatement of organic water pollutants: a critical review, *Chem. Rev.* 115 (2015) 13362–13407.
- F.C. Moreira, R.A.R. Boaventura, E. Brillas, V.J.P. Vilar, Electrochemical advanced oxidation processes: a review on their application to synthetic and real wastewaters, *Appl. Catal. B* 202 (2017) 217–261.
- M. Panizza, G. Cerisola, Direct and mediated anodic oxidation of organic pollutants, *Chem. Rev.* 109 (2009) 6541–6569.
- B. Boye, P.A. Michaud, B. Marselli, M.M. Dieng, E. Brillas, C. Comminellis, Anodic oxidation of 4-chlorophenoxyacetic acid on synthetic boron-doped diamond electrodes, *New Diamond Front. Carbon Technol.* 12 (2002) 63–72.
- B. Marselli, J. Garcia-Gomez, P.A. Michaud, M.A. Rodrigo, C. Comminellis, Electrogeneration of hydroxyl radicals on boron-doped diamond electrodes, *J. Electrochem. Soc.* 150 (2003) D79–D83.
- J. Ribeiro, F.L.S. Purgato, K.B. Kokoh, J.-M. Léger, A.R. De Andrade, Application of $\text{Ti}/\text{RuO}_2\text{-Ta}_2\text{O}_5$ electrodes in the electrooxidation of ethanol and derivatives: reactivity versus electrocatalytic efficiency, *Electrochim. Acta* 53 (2008) 7845–7851.
- O. Scialdone, S. Randazzo, A. Galia, G. Filardo, Electrochemical oxidation of organics at metal oxide electrode: the incineration of oxalic acid at $\text{IrO}_2\text{-Ta}_2\text{O}_5$ (DSA- O_2) anode, *Electrochim. Acta* 54 (2009) 1210–1217.
- B. Borbón, M.T. Oropeza-Guzman, E. Brillas, I. Sirés, Sequential electrochemical treatment of dairy wastewater using aluminium and DSA-type anodes, *Environ. Sci. Pollut. Res.* 21 (2014) 8573–8584.
- A. Thiam, E. Brillas, F. Centellas, P.L. Cabot, I. Sirés, Electrochemical reactivity of Ponceau 4R (food additive E124) in different electrolytes and batch cells, *Electrochim. Acta* 173 (2015) 523–533.
- G. Coria, I. Sirés, E. Brillas, J.L. Nava, Influence of the anode material on the degradation of naproxen by Fenton-based electrochemical processes, *Chem. Eng. J.* 304 (2016) 817–825.
- P. Cañizares, J. Lobato, R. Paz, M.A. Rodrigo, C. Saez, Electrochemical oxidation of phenolic compound wastes with BDD anodes, *Water Res.* 39 (2005) 2687–2703.
- E. Brillas, I. Sirés, C. Arias, P.L. Cabot, F. Centellas, R.M. Rodríguez, J.A. Garrido, Mineralization of paracetamol in aqueous medium by anodic oxidation with a boron-doped diamond electrode, *Chemosphere* 58 (2005) 399–406.
- C. Flox, P.L. Cabot, F. Centellas, J.A. Garrido, R.M. Rodríguez, C. Arias, E. Brillas, Electrochemical combustion of herbicide mecoprop in aqueous medium using a flow reactor with a boron-doped diamond anode, *Chemosphere* 64 (2006) 892–902.
- A. Özcan, Y. Şahin, A.S. Kopal, M.A. Oturan, Protham mineralization in aqueous medium by anodic oxidation using boron-doped diamond anode. Experimental parameters' influence on degradation kinetics and mineralization efficiency, *Water Res.* 42 (2008) 2889–2898.
- V. Santos, J. Diogo, M.J.A. Pacheco, L. Ciriaco, A. Morão, A. Lopes, Electrochemical degradation of sulfonated amines on Si/BDD electrodes, *Chemosphere* 79 (2010) 637–645.
- N. Oturan, E. Brillas, M.A. Oturan, Unprecedented total mineralization of atrazine and cyanuric acid by anodic oxidation and electro-Fenton with a boron-doped diamond anode, *Environ. Chem. Lett.* 10 (2012) 165–170.
- A. El-Ghenemy, J.A. Garrido, R.M. Rodríguez, P.L. Cabot, F. Centellas, C. Arias, E. Brillas, Degradation of sulfanilamide in acidic medium by anodic oxidation with a boron-doped diamond anode, *J. Electroanal. Chem.* 689 (2013) 149–157.
- C.I. Brinzila, N. Monterio, M.J. Pacheco, L. Ciriaco, I. Siminiceanu, A. Lopes, Degradation of tetracycline at a boron-doped diamond anode: influence of initial pH, applied current intensity and electrolyte, *Environ. Sci. Pollut. Res.* 21 (2014) 8457–8465.
- H. Olvera-Vargas, N. Oturan, E. Brillas, D. Buisson, G. Esposito, M.A. Oturan, Electrochemical advanced oxidation for cold incineration of the pharmaceutical ranitidine: mineralization pathway and toxicity evolution, *Chemosphere* 117 (2014) 644–651.
- E.V. dos Santos, C. Sáez, C.A. Martínez-Huitile, P. Cañizares, M.A. Rodrigo, The role of particle size on the conductive diamond electrochemical oxidation of soil-washing effluent polluted with atrazine, *Electrochem. Commun.* 55 (2015) 26–29.
- A. Bedolla-Guzman, I. Sirés, A. Thiam, J.M. Peralta-Hernández, S. Gutiérrez-Granados, E. Brillas, Application of anodic oxidation, electro-Fenton and UVA photoelectro-Fenton to decolorize and mineralize acidic solutions of Reactive Yellow 160 azo dye, *Electrochim. Acta* 206 (2016) 307–316.
- I. Sirés, P.L. Cabot, F. Centellas, J.A. Garrido, R.M. Rodríguez, C. Arias, E. Brillas, Electrochemical degradation of clofibric acid in water by anodic oxidation. Comparative study with platinum and boron-doped diamond electrodes, *Electrochim. Acta* 52 (2006) 75–85.
- E.B. Cavalcanti, S. Garcia-Segura, F. Centellas, E. Brillas, Electrochemical incineration of omeprazole in neutral aqueous medium using a platinum or boron-doped diamond. Degradation kinetics and oxidation products, *Water Res.* 47 (2013) 1803–1815.
- L. Ciriaco, C. Anjo, J. Correia, M.J. Pacheco, A. Lopes, Electrochemical degradation of ibuprofen on $\text{Ti}/\text{Pt}/\text{PbO}_2$ and Si/BDD electrodes, *Electrochim. Acta* 54 (2009) 1464–1472.
- C. Salazar, I. Sirés, C.A. Zaror, E. Brillas, Treatment of a mixture of chloromethoxyphenols in hypochlorite medium by electrochemical AOPs as an alternative for the remediation of pulp and paper mill process waters, *Electrocatalysis* 4 (2013) 212–223.
- A. Thiam, M. Zhou, E. Brillas, I. Sirés, Two-step mineralization of Tartrazine solutions: study of parameters and by-products during the coupling of electrocoagulation with electrochemical advanced oxidation processes, *Appl. Catal. B* 150–151 (2014) 116–125.
- A. Thiam, I. Sirés, E. Brillas, Treatment of a mixture of food color additives (E122, E124 and E129) in different water matrices by UVA and solar photoelectro-Fenton, *Water Res.* 81 (2015) 178–187.

- [38] A. Wang, J. Qu, H. Liu, J. Ru, Mineralization of an azo dye Acid Red 14 by photoelectro-Fenton process using an activated carbon fiber cathode, *Appl. Catal. B* 84 (2008) 393–399.
- [39] A. Khataee, A. Akbarpour, B. Vahi, Photoassisted electrochemical degradation of an azo dye using Ti/RuO₂ anode and carbon nanotubes containing gas-diffusion cathode, *J. Taiwan Inst. Chem. Eng.* 45 (2014) 930–936.
- [40] A. Dirany, I. Sirés, N. Oturan, A. Özcan, M.A. Oturan, Electrochemical treatment of the antibiotic sulfachloropyridazine: kinetics, reaction pathways, and toxicity evolution, *Environ. Sci. Technol.* 46 (2012) 4074–4082.
- [41] A. El-Ghenemy, R.M. Rodríguez, E. Brillas, N. Oturan, M.A. Oturan, Electro-Fenton degradation of the antibiotic sulfanilamide with Pt/carbon-felt and BDD/carbon-felt cells. Kinetics, reaction intermediates, and toxicity assessment, *Environ. Sci. Pollut. Res.* 21 (2014) 8368–8378.
- [42] I. Sirés, F. Centellas, J.A. Garrido, R.M. Rodríguez, C. Arias, P.L. Cabot, E. Brillas, Mineralization of clofibrac acid by electrochemical advanced oxidation processes using a boron-doped diamond anode and Fe²⁺ and UVA light as catalysts, *Appl. Catal. B* 72 (2007) 373–381.
- [43] J.R. Steter, E. Brillas, I. Sirés, On the selection of the anode material for the electrochemical removal of methylparaben from different aqueous media, *Electrochim. Acta* 222 (2016) 1464–1474.
- [44] F.J. Welcher, *Standard Methods of Chemical Analysis*, sixth ed, vol. 2, R.E. Krieger Publishing Co, Huntington, New York, 1975. Part B.
- [45] APWA, AWWA, WEF, *Standard methods for the examination of water and wastewater*, Method Number 4500-Cl Chlorine (residual)-G. DPD Colorimetric Method, 21st ed., American Public Health Association, Washington D.C., 2005, pp. 4-67 and 4-68.

UNCORRECTED PROOF